

## Use of a 3D printer to create a bolus for patients undergoing tele-radiotherapy

M. Lukowiak<sup>1</sup>, M. Boehlke<sup>1</sup>, D. Matias<sup>2</sup>, K. Jezierska<sup>4\*</sup>,  
M. Piątek-Hnat<sup>3</sup>, M. Lewocki<sup>1</sup>, W. Podraza<sup>4</sup>, M. El Fray<sup>3</sup>, W. Kot<sup>1</sup>

<sup>1</sup>Department of Medical Physics, West Pomeranian Oncology Center, Szczecin, Poland

<sup>2</sup>Copernicus Sp. zo.o., Szczecin, Poland

<sup>3</sup>Institute of Polymers, Department of Biomaterials and Microbiological Technology, West Pomeranian University of Technology, Szczecin, Poland

<sup>4</sup>Department of Medical Physics, Pomeranian Medical University, Szczecin, Poland

### ABSTRACT

**Background:** This study describes the possibility of implementing three-dimensional printing technology to create a precise construction of a planned bolus, based on computed tomography information stored in the Digital Imaging and Communications in Medicine (DICOM) format file. **Materials and Methods:** To create the bolus with a 3D printer, we converted data in the DICOM format to the stereolithography (STL) format. In addition, we produced a paraffin bolus that, traditionally, is manually placed directly on the patient. CT scans were acquired for both boluses, and the images were superimposed onto the patient CT scans that were used to design the bolus. The superimposition of images was performed to compare the fit of the bolus printed on a 3D printer to that of the paraffin bolus made in the traditional way. In addition, for both models, the dose distribution was simulated. To quantify the level of matching ML, special formula was used. The ML parameter had a value between 0 and 100%, where 100% indicated a perfect fit between the model and the 3D printed bolus. **Results:** We verified that 100% of the volume of the 3D printed bolus was located within the contour of the designed model. The ML of the bolus was 94%. For the classical paraffin bolus the ML was only 28%. **Conclusion:** A bolus printed on a three-dimensional printer can faithfully reproduce the structure specified in the project plan. Compared to the classical paraffin bolus, the three-dimensional printed bolus more closely matched the planned model and possessed greater material uniformity.

**Keywords:** Bolus material, 3D printing, teleradiotherapy, DICOM format, STL format.

### ► Original article

**\*Corresponding author:**

Dr. Karolina Jezierska,

Fax: +48 91 4414521

E-mail: karo@pum.edu.pl

Revised: Dec. 2015

Accepted: Jan. 2016

Int. J. Radiat. Res., October 2016;  
14(4): 287-295

DOI: 10.18869/acadpub.ijrr.14.4.287

### INTRODUCTION

The staff involved in the process of teleradiotherapy is required to implement procedures with high quality assurance. The implementation of the treatment plan for clinical use is particularly important. This importance follows from the uncertainty related to the reconstruction of patient positioning or the production of accessories specified individually

for each patient in the treatment planning system, which can affect the final therapeutic effect <sup>(1-3)</sup>. Technological advances in radiotherapy have facilitated the reduction of errors related to the reconstruction of patient geometry, but errors remain in the production of accessories required to implement advanced modeling.

The primary accessory is the bolus, which is a material used to compensate for unevenly

shaped tissues in the patient. The purpose of the bolus is to provide additional absorption and to scatter ionizing radiation to achieve greater dose homogeneity around the irradiated tumor. This very important accessory is engineered in a planning system, based on computed tomography (CT) scans of the patient, acquired for the purpose of treatment planning.

In photon radiation, the only reason to use a bolus is to shift the build-up region (in the

direction of the radiation beam) to ensure maximum dose at the tumor area.

For electron beams, a bolus is used mainly for two reasons. First, a bolus is used to reduce dose inhomogeneity, which results from surface curvature. The dose may become focused or diffused, when the surface is not flat (figure 1). Second, a bolus is used to match the electron range to the depth of the tumor, and thus, limit the damage to healthy tissue situated behind the tumor.

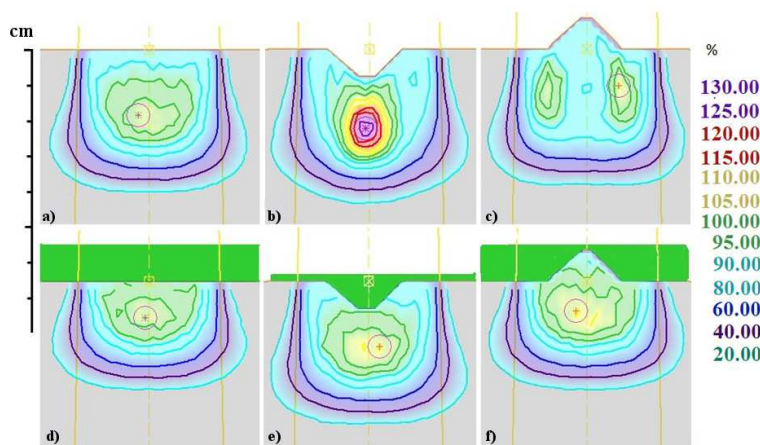


**Figure 1.** For an electron beam, the bolus reduces dose inhomogeneity. a) An example of a dose distribution for an electron beam of 9 MeV, which irradiates a field of 4×4 cm. b) A dose distribution for the same beam, modified by the gap in the phantom (the skin surface). Below the gap, the dose is significantly increased (in this geometry, by about 25%). c) A dose distribution for the same beam, modified by the convex surface in the phantom (the skin surface). Below the convex region, the dose is decreased (in this geometry, by about 20%). d) A dose distribution modified by a bolus between the tissue and the electron source. The range of electrons in the phantom (the tissue) is reduced by the thickness of the bolus. The build-up region is moved into the bolus, which increases the dose at the phantom surface (skin surface) to a value near 100%. e) A dose distribution modified by using a bolus that fills the surface gap. The region of high dose disappears. f) A dose distribution modified by using a bolus that compensates for the surface bulge. The region of reduced dose disappears. In addition, the range of electrons in the phantom (the tissue) is reduced.

Any change in the shape of a bolus may affect the dose distribution in the tumor area. This could impede achievement of the dose coverage of a target volume. To control radiation absorption and scattering in the bolus, it is typically constructed with materials that have a density similar to the density of soft tissue, approx. 1 g/cm<sup>3</sup>. There are many materials that can be used to create a bolus (4-7). The problem is to reconstruct accurately the structure of the patient's body. Based on our experience in tissue engineering for creating model structures of tissues or whole organs, we reasoned that the precise structure of a bolus could be obtained with three-dimensional (3D) printing technology

and produced with a 3D printer (8-9).

This study aimed to implement 3D printing technology to create a bolus that precisely fit an anatomical structure, based on CT information stored in DICOM format. Although recently there have been several reports describing the possibility to implementation of the three-dimensional printing technology to produce bolus in radiotherapy, this is still a new and very rarely used method (10-11). Presumably, boluses printed in this technology are nowhere routinely used in radiation therapy. The presented work is probably the only such research in Europe till now. First of all, it is due to the difficulties associated with the lack of

commercial software that can generate a file with the shape of a bolus in a format read by the 3D printer. The second reason is the lack of a medical certificates for materials commercially used in 3D printers, so the consent of the ethics committee for the use of the 3D bolus in clinical practice is prerequisite.

## MATERIALS AND METHODS

This study included one patient qualified for treatment in the West Pomeranian Oncology Center in Szczecin. The patient required a bolus, due to a tumor on the skin surface, located in the corner of the left eye. The therapy regimen assumed application of a total therapeutic dose of 60 Gy, delivered in 30 fractions. All targets and organs at risk had been drawn on the CT images, which were acquired at 2-mm intervals.

The radiation dose distribution was calculated and analyzed with the Nucletron Oncentra MasterPlan system, version 4.3., used a Voxel Monte Carlo calculation algorithm and set the number of trials to 50,000/cm<sup>2</sup>. Calculations were performed with a 2.0-mm grid. The homogeneity of the dose distribution was evaluated based on the criteria from the International Commission on Radiation Units

and Measurements (Report 50)<sup>(12)</sup>. Protection of normal tissues was planned in accordance with guidelines established as the Quantitative Analysis of Normal Tissue Effects in the Clinic. The treatment plan included the application of a single electron beam with an energy of 9 MeV. To obtain a uniform dose distribution around the tumor, we used CT scans of the patient to design a bolus with a density of 1 g/cm<sup>3</sup>. Its thickness was determined by the range of electrons in the material (energy 9 MeV).

To create the bolus with a 3D printer, we converted data in the DICOM format to the stereolithography (STL) format, which is supported by the 3D printer. The DICOM file format contained information about the shape of the bolus on each scanned layer, specified as a set of vertices defined in a space with x, y, and z coordinates.

Conversion of DICOM file into the STL format supported by the 3D printer was achieved by connecting each layer of the bolus into a 3D triangulation structure (figure 2). The 3D STL structure was generated with software developed for the purpose. The bolus was divided into layers, spaced 2-mm apart. These layers were connected together with triangles, where a single section from one layer was joined to two vertices on the adjacent layer.

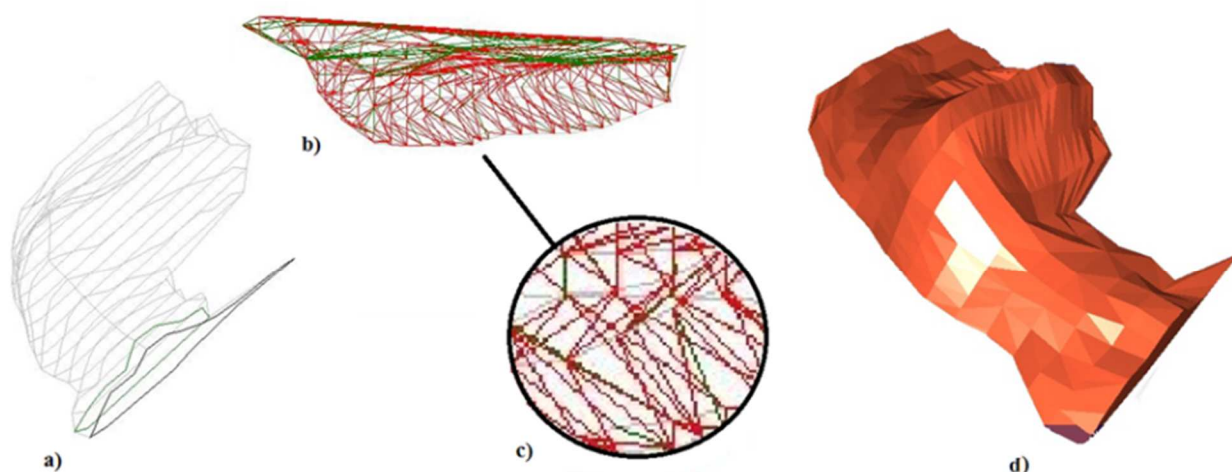


**Figure 2.** Conversion of DICOM data to STL format. a) A series of bolus layers imported from patient CT data saved in the DICOM file. b) Connection of the individual layers with 3D triangular structures; this data is saved in STL format; c) Magnified section shows how triangles connect the individual layers; d) Reconstructed model of the bolus created in the system supported by a 3D printer.

In addition, we produced a paraffin bolus that, traditionally, is manually placed directly on the patient. In the classical method, the treatment planning system divided the bolus structure into a number of longitudinal, 1, 5-mm thick layers (corresponding to the thickness of one slice of paraffin). Based on the diagram created by planning system, the specified layers of bolus were cut from paraffin and placed on the body of the patient.

CT scans were acquired for both boluses, and the images were superimposed onto the patient CT scans that were used to design the bolus. The superimposition of images was performed to compare the fit of the bolus printed on a 3D printer to that of the paraffin bolus made in the traditional way. In addition, for both models, the dose distribution was simulated. Flowchart (figure 3) presents the major steps in the process.

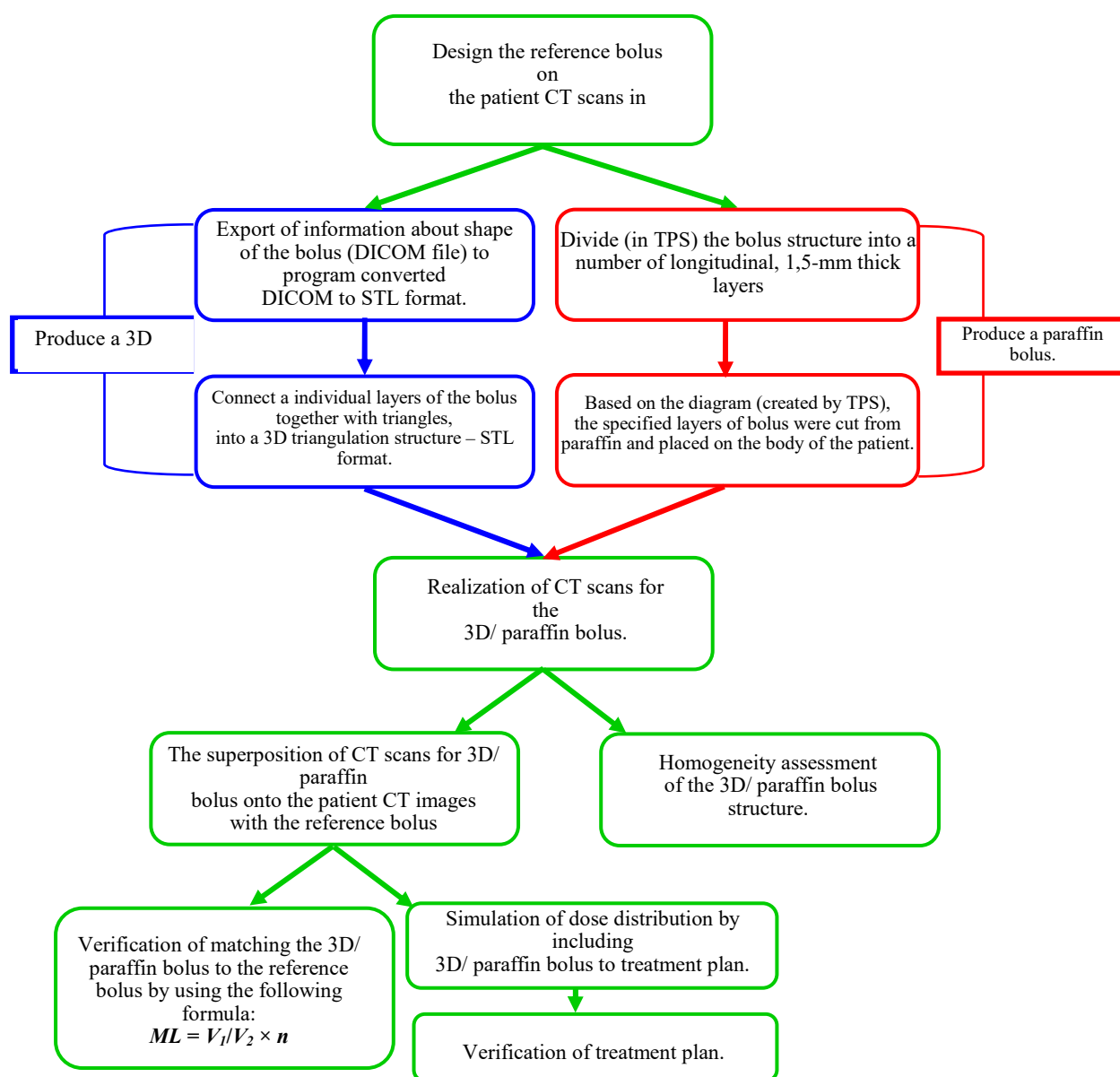


Figure 3. Flowchart of boluses preparation process. TPS – treatment planning system.

The printed bolus was created with a 3D CB-printer, which implemented Fused Deposition Modeling (FDM) technology. FDM is based on the layered deposition of melted material. The bolus was divided into 100- $\mu$ m thick layers; corresponding support structures were included in the layers, when required by the shape of the bolus. Then, according to the 3D model saved in STL format, paths were defined to determine the stacking of the specified layers of building material. To control the printer, we used the software program, Repetier-Host version V1.0.6. To obtain uniform cross-sections, 100% filling print was applied.

The material used to print the 3D bolus was a copolymer acrylonitrile-butadiene-styrene (ABS) with a density equivalent to soft tissue (1.05 g/cm<sup>3</sup>) and a chemical composition close to the chemical composition of the human body. ABS had the appropriate mechanical properties; its main advantages were high resilience and abrasion resistance. Additionally, the analyzed material was toxicologically and biologically neutral.

To investigate the influence of ionizing radiation on the analyzed material, two plates with an area of 10×10 cm and a thickness of 1 mm were tested. One plate was irradiated with a 60 Gy dose (therapeutic dose received by the patient) and the other plate was untreated. The plates were evaluated with the differential scanning calorimetry (DSC) method and data were recorded with a DSC Q100 (TA Instruments) apparatus. The plates were

subjected to a triple cycle (heating-cooling-heating) in the temperature range of -90 °C to +250 °C. The heating and cooling rates were 10 °C/min. Quasi-static tensile data were collected at room temperature with an Instron 3660 tensile tester, equipped with a 500-N load cell, which employed a crosshead speed of 10 mm/min. The strain was measured in terms of clamp displacement, according to PN-ISO 527-1:1998. The starting clamp distance was 25 mm. The results are expressed as the average from 5 specimens with cross sections of 0.5 × 4 mm.

The level of matching between the 3D printed bolus and the model designed in the treatment planning system was examined in superimposed CT cross-sections (figure 4). To quantify the level of matching (*ML*), the formula (5) was used:

$$ML = V_1/V_2 \times n \quad (1)$$

Where;  $V_1$  is the volume of the test bolus contained within the designed model contour;  $V_2$  is the total volume of the model bolus; and  $n$  is the percent of test bolus contained within the contour of the model. The *ML* parameter had a value between 0 and 100%, where 100% indicated a perfect fit between the model and the 3D printed bolus. Presented *ML* formula was developed by the authors and it is based on the coverage index, parameter commonly used in radiotherapy to assess the degree of target irradiation (13, 14). The formula allows a quantitative estimation of the degree of alignment of the tested bolus (3D or paraffin) to the reference model.

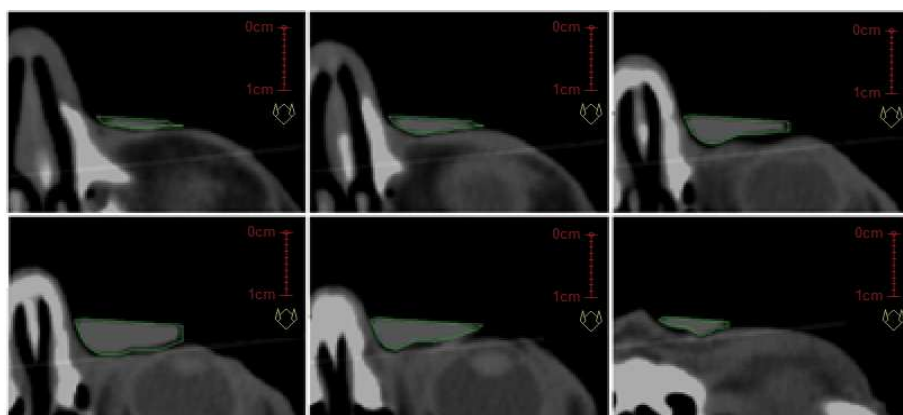


**Figure 4.** Selected cross-sections of superimposed CT scans show the matching between the 3D printed bolus and the model design. The CTs of the patient were superimposed with scans of the 3D printed bolus. The green contour marks the shape of the model bolus designed in the Oncentra MasterPlan system.



## RESULTS

Based on the information obtained from the Oncentra MasterPlan system, we verified that 100% of the volume of the 3D printed bolus was located within the contour of the designed model ( $V_2=1.43 \text{ cm}^3$ ). The total volume of the 3D printed bolus was slightly smaller than the model ( $V_1 = 1.35 \text{ cm}^3$ ). The *ML* of the bolus was 94%.

For comparison, we examined the level of matching for the classical paraffin bolus (figure 5) and we calculated the *ML* for the paraffin bolus. Based on information obtained from the Oncentra MasterPlan system, we verified that  $1.02 \text{ cm}^3$  of the paraffin bolus volume was located within the contour of the designed model. The total volume of the paraffin bolus was larger than the model ( $V_1 = 2.64 \text{ cm}^3$ ). However, in this case, the *ML* was only 28%.

An important factor shown in the CT scans was that the structure of the 3D printed bolus

was more uniform than that of the paraffin bolus produced with the classical method. The paraffin bolus contained air cavities that are undesirable for an electron beam, because they may affect the flow of electrons passing through the bolus material.

Furthermore, based on a dose volume histogram, the therapeutic dose received by the target volumes were evaluated for the different bolus types (table 1). Compared to the designed model, the 3D printed bolus showed slight differences in dose distribution, and the paraffin bolus showed a significantly more heterogeneous dose distribution. Differences in the coverage of the target volume with a 95% isodose ranged from 1.7 to 7%, compared to the reference plan. The different dose distributions achieved with the different bolus types were examined at selected cross-sections to determine the target volume coverages (figure 6).

The effect of radiation on the thermal properties of the ABS polymer were examined by

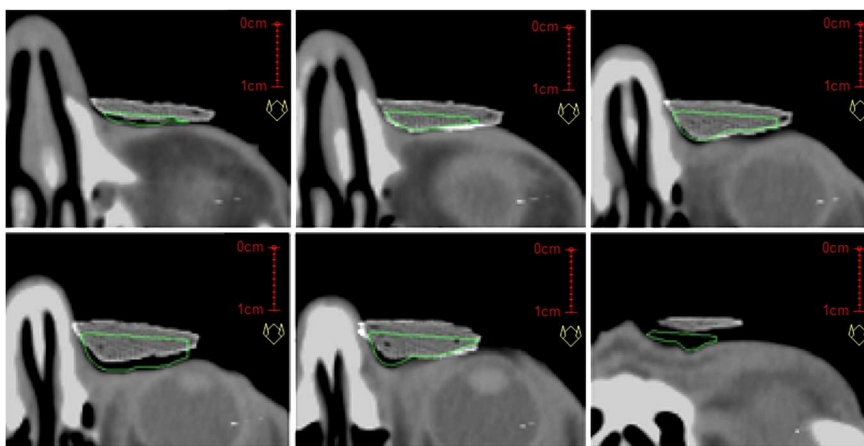


**Figure 5.** Selected cross-sections of superimposed CT scans show the matching between the paraffin bolus (placed on the skin of the patient) and the model design. The CTs of the patient were superimposed with scans of the paraffin bolus. The green contour marks the shape of the model bolus designed in the Oncentra MasterPlan system bolus.

**Table 1.** The percentage differences in dose distributions compared to the treatment plan with the designed model bolus. GTV - the gross tumour volume, CTV - the clinical target volume, PTV - the planning target volume.

| Targets | Type of bolus  | Dmin[%()] | Dmean[%()] | Dmax[%()] |
|---------|----------------|-----------|------------|-----------|
| GTV     | bolus 3D       | 0,39      | 0,37       | 1,41      |
|         | paraffin bolus | 4,01      | 1,40       | 8,56      |
| CTV     | bolus 3D       | 0,44      | 0,09       | 1,63      |
|         | paraffin bolus | 1,67      | 0,63       | 2,10      |
| PTV     | bolus 3D       | 0,62      | 0,08       | 1,63      |
|         | paraffin bolus | 7,36      | 0,57       | 2,10      |

DSC (figure 7). DSC thermograms measured before and after a dose of 60 Gy showed the glass transition associated with the amorphous phase of the ABS polymer. The value of the glass transition temperature did not change, indicating that the radiation dose did not affect the thermal properties of the ABS polymer. Observed no effect dose of 60 Gy on thermal properties is related to the chemical structure of

the ABS and the presence of the benzene ring, which causes the polymer very resistant to ionizing radiation, as described in the literature (15).

We also compared the mechanical properties of ABS before and after irradiation with 60 Gy (figure 8). Tensile strength only slightly changed, but the elasticity decreased in the higher values of the Young's modulus.

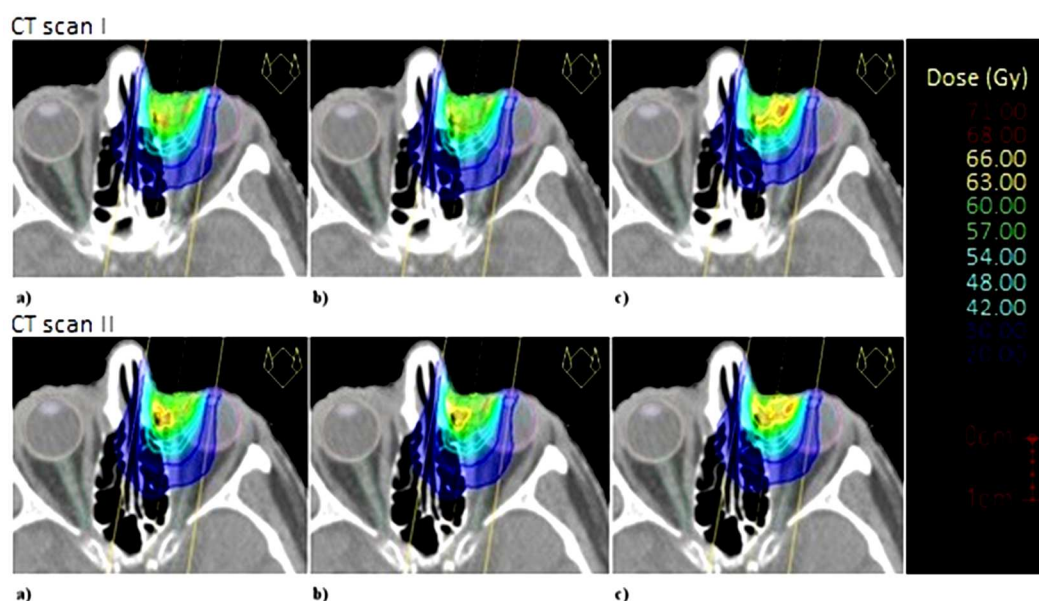


**Figure 6.** Dose distribution and coverage of the target volume. Representative images show dose distributions by implementing a) the reference plan, b) the 3D bolus, and c) the paraffin bolus.

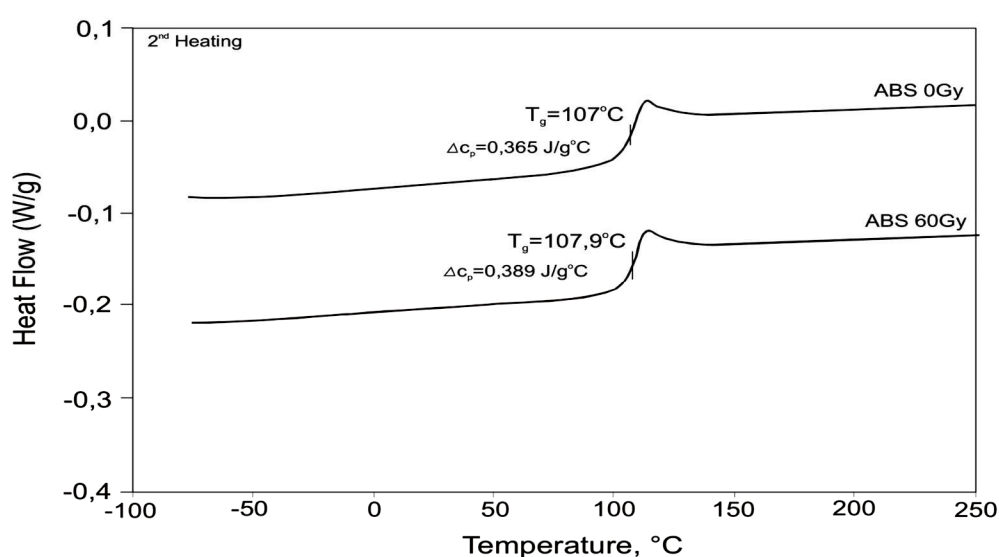


**Figure 7.** DSC 2nd heating thermograms measured before and after irradiation of the ABS polymer.  $T_g$  is the glass transition temperature and  $\Delta c_p$  is change in the heat capacity of polymer.

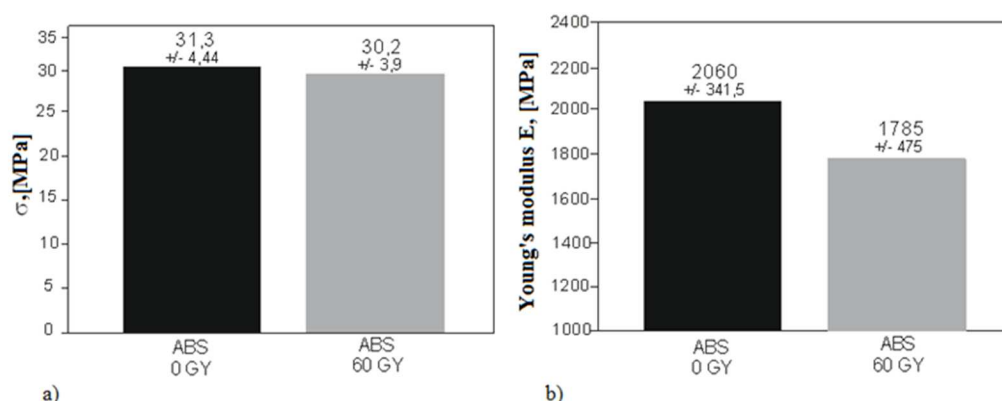


**Figure 8.** Mechanical properties of the ABS polymer before and after irradiation. a) Tensile strength  $\sigma$  and b) elasticity measured with Young's modulus  $E$ .

## DISCUSSION

The use of 3D printing technology to recreate a bolus designed in a treatment planning system can increase the quality of teleradiotherapy <sup>(10)</sup>. This paper showed that a 3D printed bolus represented a precise reproduction of the designed model bolus at relatively low cost. This precision increased the certainty that the dose distribution in the target area would be consistent with the planned dose distribution and results a substantial reduction of the volume of normal tissues being irradiated, which agrees with the results of Su *et al.* <sup>(10)</sup>. The 3D printed bolus displayed a better fit to the planned model and greater material uniformity compared to the classical paraffin bolus. Although the structure of a classical bolus can be directly molded by placing it on the tissue of a patient, this tissue can be easily deformed; thus, the paraffin bolus did not precisely reproduce the planned bolus. Moreover, application of the individual paraffin layers caused undesirable air cavities, which can affect the flow of electrons passing through the material. This inhomogeneity can change the dose distribution relative to the planned distribution. Using 3D printed bolus could help to overcome the problem with air cavities and improve the quality of realized treatment, by reproducibility of daily setup conditions on irregular surfaces, which was confirmed by Shin-Wook *et al.* <sup>(11)</sup>. Additionally, a 3D printer can be easily installed in the cancer center and offer practical advantages - neither patient nor staff

needs to be present all the time during the bolus production, which was confirmed by Su *et al.* <sup>(10)</sup>.

Importantly, for clinical applications, we found that the radiation dose had little effect on the thermal and mechanical properties (glass transition temperature, tensile strength and Young's modulus) of the ABS polymer.

The simulation results of other studies showed that it is possible to create boluses with variable shapes, location, and proximity to the organs at risk <sup>(10)</sup>. Therefore in the future, 3D printing technology may become a valuable, relatively inexpensive tool for supporting in teleradiotherapy and we expect to adopt this methodology into our clinical practice.

**Conflict of interest:** Declared none.

## REFERENCES

1. Jomehzadeh A, Shokrani P, Mohammadi M, Amouheidari A (2014) A quality assurance program for an amorphous silicon electronic portal imaging device using in-house developed phantoms: a method development for dosimetry purposes. *Int J Radiat Res*, **12(3)**: 257-64.
2. Chang-li R, Yu-xin C, Lu-zhou W, U-bing W, Song Q (2015) The influence of respiratory motion on dose distribution of 3D-CRT and IMRT- A simulation study. *Int J Radiat Res*, **13(1)**: 39-43.
3. Aghahadi B, Zhang Z, Zareh S, Sarkar S, Tayebi PS (2006) Impact of quality control on radiation doses received by patients undergoing abdomen X-ray examination in ten hospitals. *Iran JRR*, **3(4)**: 177-82.
4. Łukowiak M, El Fray M, Piątek-Hnat M, Lewocki M (2015) Polymers in teleradiotherapy. *IFM*, 1/2015: 29-32.



5. Babic S, Kerr AT, Westerland M, Gooding J, Schreiner LJ (2002) Examination of Jeltrate Plus as a tissue equivalent bolus material. *J Appl Clin Med Phys*, **3(3)**: 170-5.
6. Huang KM, Hsu CH, Jeng SC, Ting LL, Cheng JC, Huang WT (2006) The application of Aquaplast Thermoplastic as a bolus material in the radiotherapy of a patient with classic Kaposi's sarcoma at the lower extremity. *Anticancer Res*, **26(1B)**: 759-62.
7. Montaseri A, Ay MR, Mahdavi R (2012) Physical properties of ethyl methacrylate as a bolus in radiotherapy. *IJMP*, **9(2)**: 127-34.
8. Avelino SR, Silva LFO, Miosso CJ (2012) Use of 3D-Printers to Create Intensity-Modulated Radiotherapy Compensator Blocks. *Conf Proc IEEE Eng Med Biol Soc*, **2012**: 5718-21.
9. Ju SG, Kim MK, Hong CS, Kim JS, Han Y, Choi DH, Shin D, Lee SB (2014) New technique for developing a proton range compensator with use of a 3-dimensional printer. *Int J Radiat Oncol Biol Phys*, **88(2)**: 453-8.
10. Su S, Moran K, Rorbar JL (2014) Design and production of 3D printed bolus for electron radiation therapy. *JACMP*, **15(4)**.
11. Kim SW, Shin HJ, Kay CS, Son SH (2014) A customized bolus produced Using a 3 – dimensional printer for radiotherapy. *PLoS One*, **9(10)**: e110746.
12. ICRU Report 50 (1993) Prescribing, Recording and Reporting Photon Beam Therapy. International Commission on Radiation Units and Measurements, Bethesda, USA, 1993.
13. Baldock C, Lepage M, Bäck SAJ, Murry PJ, Jayasekera PM, Porter D, Kron T (2001) Dose resoluon in radiotherapy polymer gel dosimetry: effect of echo spacing in MRI pulse sequence. *Phys Med Biol*, **46(2)**: 449-60.
14. Musat E, Kantor G, Caron J, Lagarde P, Laharie H, Stoeckle E, Angles J, Gilbeau L, Bui BN (2004) Comparison of intensity-modulated postoperative radiotherapy with conventional postoperative conformal radiotherapy for retroperitoneal sarcoma. *Cancer Radiother*, **8(4)**: 255-61.
15. Ishigaki I and Yoshi F (1992) Radiation Effects on Polymer Materials in Radiation Sterilization of Medical Supplies. *Radiat Phys Chem*, **39(6)**: 527-33.

